Journal Pre-proof

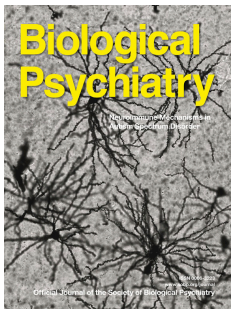

Social synchronization of conditioned fear in mice requires ventral hippocampus input to amygdala

Wataru Ito, Alexander J. Palmer, Alexei Morozov

PII: S0006-3223(22)01444-5

DOI: https://doi.org/10.1016/j.biopsych.2022.07.016

Reference: BPS 14938

To appear in: *Biological Psychiatry*

Received Date: 14 December 2021

Revised Date: 17 June 2022

Accepted Date: 11 July 2022

Please cite this article as: Ito W., Palmer A.J. & Morozov A., Social synchronization of conditioned fear in mice requires ventral hippocampus input to amygdala, *Biological Psychiatry* (2022), doi: https://doi.org/10.1016/j.biopsych.2022.07.016.

Social synchronization of conditioned fear in mice requires ventral hippocampus input to amygdala

Wataru Ito*, Alexander J. Palmer, Alexei Morozov*

Fralin Biomedical Research Institute at Virginia Tech Carilion, Roanoke, VA, USA

*Correspondence: 2 Riverside Circle, Roanoke, VA, 24016, wataru.ito@gmail.com or alexeim@vtc.vt.edu

Running title: Emotional synchronization in mice

Keywords: conditioned fear; threat response; behavioral synchronization; hippocampus; amygdala; mice

Abstract

Background: Social organisms synchronize behaviors as an evolutionary-conserved means for thriving. Synchronization under threat, in particular, benefits survival and occurs across species, including humans, but the underlying mechanisms remain unknown, due to the scarcity of the relevant animal models. Here, we developed a rodent paradigm in which mice synchronize classically conditioned fear response and identified an underlying neuronal circuit.

Methods: Males and female mice were trained individually in an auditory fear conditioning and then tested 24 h later as dyads allowing unrestricted social interaction during exposure to the conditioned stimulus, under the visible or infrared illumination to eliminate visual cues. The synchronization of the immobility or freezing bouts was quantified by calculating the effect size Cohen's D for the difference between the actual freezing time overlap and the overlap by chance. The inactivation of the dorsomedial prefrontal cortex, dorsal hippocampus, or ventral hippocampus was achieved by local infusions of muscimol. The chemogenetic disconnection of the hippocampus-amygdala pathway was performed by expressing hM4D(Gi) in the ventral hippocampal neurons and infusing CNO in the amygdala.

Results: Mice synchronized cued but not contextual fear. It was higher in males than in females and attenuated in the absence of visible light. Inactivation of the ventral but not dorsal hippocampus or dorsomedial prefrontal cortex abolished fear synchronization. Finally, the disconnection of the hippocampal-amygdala pathway diminished fear synchronization.

Conclusions: Mice synchronize expression of conditioned fear relying on the ventral hippocampus-amygdala pathway, suggesting that the hippocampus transmits social information to the amygdala to synchronize threat response.

Introduction

From invertebrates to humans, social organisms coordinate various activities, including defense from predators, foraging, raising progeny, and migration (1-5). One simple form of coordination is aligning of movement (1, 6). In humans, it is called nonverbal interpersonal synchrony is an indicator of social normality. It correlates with prosocial behaviors; it is increased by oxytocin, and decreased in schizophrenia, borderline personality disorder, and autism (7-13).

While many species coordinate body movement (1), only few publications report such coordination in rodents. For example, rats shuttle together to obtain reward in an operant task (14) and aggregate in response to predator smell or bright light (15-17). Mice aggregate in the presence of a spider-robot, and being inside the aggregation attenuates the threat-induced gamma oscillations in the amygdala (18). Prairie voles follow the leader-animal to generate a uniform response to an owl attack (19-21). The few examples of coordinated threat responses suggest that rodents can be used to study basic mechanisms of emotional synchronization. Although the mouse is a gregarious species with robust social modulation of threat responses (22-27), no study has established a quantitative paradigm for social synchronization of threat response in mice. Here, we provide such a paradigm based on the classical Pavlovian conditioning and identify a neuronal circuit essential for synchronization of classically conditioned fear response.

Methods and Materials

All experiments were performed according to a Virginia Tech IACUC-approved protocol.

Animals

Breeding trios of one C57BL/6N male and two 129SvEv females produced 129SvEv/C57BL/6N F1 hybrid male and female mice weaned at p21 and housed four littermates per cage with the same sex as described (23). Subjects underwent tests at p75-p90. 7-10 days before testing, mice were split two per clean cage with a quarter of the Nestlet material from the originating cage.

Fear conditioning

Mice in each dyad were trained independently in two separate conditioning chambers (Med Associates, St. Albans, VT) as described (28) and then tested together as dyads in a single chamber. For cued fear training, each animal spent the first 2 min in the chamber without stimuli and then received four pairings of the conditioned stimulus (CS) and unconditioned stimulus (US) given in variable intervals (60-180 s). The CS was a 30 s, 8 kHz, 80 dB tone, and the US was a 0.5 mA 0.5 s electrical shock co-terminated with CS. Mice returned to the home cage 30 s after the last CS-US pairing. Cued fear was tested once one day later or twice one day and three days later in the DREADD experiments and in the muscimol inactivation of vHPC in Fig3. First, the animals spent 1 min in a new context without CS and 2 min with CS. For contextual fear training, each animal spent 2.5 min in the chamber without stimuli and then received three 0.8 mA 2 s footshocks separated by 1 min and returned to the home cage 30 s after the last shock. Contextual fear was tested one day later by placing the dyads in the training chamber for 3 min. Videos were recorded at four frames per second, exported as AVI files with MJPEG compression using the Freezeframe system (Actimetrics, Wilmette, IL), and then converted to the mp4 format using a Python script.

Quantification of freezing, freezing overlap, freezing synchrony, and leader-follower relationship.

Annotators, unaware of the treatment of the animals, manually identified and recorded the first and last video frames of each freezing bout using a Python script. A freezing bout was defined as the lack of movement except for respiration for at least four consecutive video frames. From the annotation, another Python script generated freezing duration for each animal, freezing overlap for each dyad (duration of simultaneous freezing), and graphic representation of their temporal dynamics. We defined freezing synchrony as the standardized difference (Cohen's D effect size) between the observed and chance freezing overlaps. The chance overlaps were obtained by

performing 1000 random circular permutations of the freezing timelines and computing the freezing overlap for each. The synchrony was obtained by subtracting the mean of chance overlaps from the observed overlap and dividing it by the standard deviation of chance overlaps. To evaluate the leader-follower relationship within each dyad, we calculated the "leadership bias" and "% maximum leadership." First, dyad members were assigned arbitrarily as #1 and #2 (Fig3BC), or specifically as #1 for the cannulated and #2 for the non-cannulated member (Fig3DE). Then, we counted the matched transitions, in which one animal (follower) followed another (initiator), and summated the counts as the "leadership bias" using +1 when subject #1 was the initiator and -1 for subject #2 as the initiator (FigS14). In the case of perfect leadership, where one member always takes the leadership, the absolute value of the "leadership bias" equals the total number of the matched transitions (theoretical maximum). To standardize the leadership measure across dyads, we expressed leadership bias as % of theoretical maximum (% maximum leadership) at the end of the test session. The signed "% maximum leadership" identifies the leader animal (positive for subject #1 and negative for subject #2).

Surgeries and intracranial infusions

Viral injections. Pseudotype 5 viral vectors pAAV-hSyn-hM4D(Gi) (Addgene), pAAV-hSyn-EGFP (Addgene) or pAAV-hSyn-Chronos-GFP (UNC Vector Core) at the titer of 10^{12} viral particles per mL were injected bilaterally in two locations, 0.2 µL per site, targeting the intermediate hippocampus (from bregma: -3.4 mm posterior, ±3.4 mm lateral; from the brain surface: -1.65 mm ventral) and ventral hippocampus (from bregma: -3.4 mm posterior, ±3.8 mm lateral; from the brain surface: -2.6 mm ventral) following the surgical procedure described in (29).

Cannulation. Ten to 14 days before fear conditioning, mice received implantation bilaterally with guide cannulas, made in the lab from hypodermic tubes or purchased from Plastic One (Roanoke, VA) to target dmPFC (from bregma: 1.5 mm anterior, ±0.5 mm lateral, from the brain surface: -0.8 mm ventral), vHPC (from bregma: -3.3 mm posterior, ±3.3 mm lateral, from the brain surface

-2.8 mm ventral) or BLA (from bregma: -1.8 mm posterior, ±3.2 mm lateral, from the brain surface -3.5 mm ventral). Dummy cannulas were placed in the guide cannulas to prevent clogging.

Intracranial infusion. During seven days before testing, animals were handled for 2-3 min daily, including removal and reattachment of dummy cannulas. One day before fear conditioning training, mice were habituated to infusion using the vehicle: (in mM) 150 NaCl, 10 D-glucose, 10 HEPES, 2.5 KCl, 1 MgCl2, pH 7.35 (30) in the home cage in the presence of the partner. The infusion cannula extended 1 mm over the guide cannula. The infusion volume was always 150 nL per site, and the infusion rate was 75 nL/min. Muscimol (1.17 mM) or vehicle were infused one hour before fear testing. In DREADD experiments, the infusate was CNO (3 μM) or vehicle, infused 45-50 min before testing. In all experiments, except in Fig3DE, both mice in the same dyad received identical infusions.

Position verification for cannulas and viral transduction. After the final test, each animal, anesthetized with 2.5% Avertin (prepared by mixing 10 g of 2,2,2-tribromoethyl alcohol (Aldrich T4,840-2) with 10 ml of tert-amyl alcohol (Aldrich 24,048-6), diluting 1:40 by PBS and filter-sterilization), received an intracranial infusion of Chicago Sky Blue (0.2 %), followed by transcardial perfusion with 4% paraformaldehyde. Fluorescent and visible light microscopy identified the sites of viral transduction and cannulation.

Whole-cell recording

Slice preparation and whole-cell recording from amygdala neurons were done as described in (31). Briefly, the internal solution of the recording pipette was 120 K-gluconate (in mM), 5 NaCl, 1 MgCl2, 10 HEPES, 0.2 EGTA, 2 ATP-Mg, and 0.1 GTP-Na. 470 nm 1 ms light pulses from an LED lamp (Thorlabs) through a ×40 objective lens (Olympus, Center Valley, PA) stimulate the hippocampal axons expressing Chronos at 0.3 to 2.5 mW every 30 sec. Stimulus intensity was adjusted to obtain EPSCs at about 80% of the maximum.

Data analysis

Statistical analyses were performed using GraphPad Prism 5 (GraphPad Software, La Jolla, CA) and Python scripts using SciPy statistical functions (scipy.stats), and R. Normality was tested using the Shapiro–Wilk test (TableS3). Datasets with normal distribution were compared using the one-sample t-test or the paired t-test as indicated. The datasets with non-normal distribution were compared using the Mann–Whitney test, the Wilcoxon matched-pairs test, and the Wilcoxon signed-rank test. All the tests were two-sided. The two-tailed p-value was calculated for the Spearman correlation analysis. The effects were deemed significant with $p < 0.05$. The effect size as a bootstrap 95% confidence interval (CI) was computed and plotted using the data analysis with bootstrap-coupled estimation (DABEST) in Python 1(32). For each comparison, 5000 reshuffles of each group were performed.

Data and code availability

All primary data, including video files, are available from authors upon reasonable request. In addition, codes for data analysis and statistics are provided with example data as part of the replication package. It is available at https://github.com/wataruito/codes_in_Emotional_sync_Ito_et_al.

Results

To study synchronization of fear response, we trained mice individually and then tested them in dyads of cage-mates on the following day. During training, repeated auditory conditioned stimuli (CS) were paired with electrical footshocks as the unconditioned stimulus (US). During testing, mice were allowed unrestricted social interaction while exposed to CS in a different context (Fig1A). To quantify synchrony of freezing within each dyad, we calculated the Cohen's D effect size for the simultaneous freezing above chance. As shown in Fig1C, the difference between the

observed freezing overlap (L) and the mean of permutation-generated freezing overlaps (C: chance overlap) was divided by the standard deviation (SD) of the chance overlaps (Fig1B, C).

Both sexes synchronized freezing but males synchronized more than females (Fig1D, left). In males, synchrony did not correlate with the following freezing measures: % freezing average, % freezing of the high freezer, % freezing of the low freezer, and the difference of % freezing between high and low freezers (Fig1E, FigS1), the mean duration, or the number of freezing bouts (FigS3, TableS2). In females, synchrony also did not correlate with all freezing measures except a weak correlation with % freezing of the low freezer (R^2=0.3, p=0.03) (Fig1G, FigS1) and the mean duration of freezing bouts (FigS3, TableS2).

Visual, auditory, olfactory, and somatosensory social cues can convey information about the partner's state. Testing dyads under infrared illumination aimed to examine the role of vision. Most males failed to synchronize, whereas most females synchronized (p=0.048) (Fig1D, right), and there was a significant sex*lighting interaction (F(1,57)=7.0, p=0.015). The freezing under the infrared light was lower in both sexes (males: p<0.0001, females: p=0.005) (Fig1E-H), consistent with earlier findings (33). Nevertheless, synchrony did not correlate with the freezing measures (Fig1F, H, FigS1).

To examine synchronization of contextual fear, we trained a separate cohort of males by exposure to electrical footshocks and tested them in the training context 24 h later. Unlike cued freezing, mice did not synchronize bouts of contextual freezing (FigS12). Notably, in all the above cohorts, freezing strongly correlated between partners regardless the level of fear synchrony (FigS2, TableS1).

In search of the brain regions involved in synchronization, we focused on three areas, the dorsomedial prefrontal cortex (dmPFC), dorsal hippocampus (dHPC), and ventral hippocampus (vHPC). They all encode social information (34-37), contribute to social memory (37) and modulate fear expression (22, 38-41). Therefore, each structure can contribute to integrating social and emotional information required for synchronized freezing. To this end, each structure

was inactivated by bilateral muscimol infusion (Fig2A, B, E, H) in both animals of each dyad 1 h before testing. These experiments were performed on males because males synchronized stronger than females. The vHPC inactivation diminished synchrony without affecting freezing (Fig2I, J) and duration or number of freezing bouts (FigS5). Whereas inactivation of dHPC or dmPFC did not attenuate synchrony but decreased freezing (Fig2C, F), consistent with the described effects of such inactivation on fear expression (38, 42-44). In all experiments, synchrony did not correlate with freezing measures of the dyad (Fig2D, G, J, FigS4).

To confirm the role of vHPC in synchrony and examine how vHPC determines the leader of the freezing transitions, we repeated the muscimol infusion experiments but used within the dyad comparisons to absorb the effects of variability among individual dyads. After training, all dyads were tested twice: 24h (TEST1) and 72h (TEST2) later. We ran two independent cohorts: both dyad members received muscimol or vehicle infusion in vHPC (cohort #1), or only one member received the infusions (cohort #2). The order of infusion was counterbalanced between muscimol and vehicle (Fig3A). The repeated testing *per se* caused fear extinction but no effects on synchrony (FigS8). Muscimol significantly decreased synchrony in cohort #1 (Fig3B), reconfirming that vHPC is needed for synchrony, but not in cohort #2 (Fig3D), indicating that synchrony remains when one of the animals has a functional vHPC. Muscimol had no effect on % freezing or duration and number of freezing bouts (FigS7), and synchrony did not correlate with freezing measures (Fig3B, 3D, FigS6).

Next, we calculated the “leadership bias” as a metric of which dyad member and how much takes more leadership, and the “% maximum leadership” as the normalized leadership bias. In the case of the perfect leadership, when subject #1 or #2 leads all freezing transitions, the leadership bias is + (total transition number) or – (total transition number), and the % maximum leadership is +100% or -100%, respectively (explained in Methods and Materials and FigS14).

Among the two cohorts, in 73.8% of test sessions (31 out of 42), the % maximum leadership was below 30 %, and there was little or no progressive increase of the absolute

leadership bias along with the transition number (Fig3C, E, left and middle, solid lines), indicating the lack of strong leaders. However, muscimol infusion increased the number of dyads with higher % maximum leadership (above 30 %) from 1 to 5 in cohort #1 and from 1 to 4 in cohort #2 (Fig3C, E, left and middle, broken lines). When only one mouse received muscimol (cohort #2), that mouse took more leadership, as shown by significantly increased % maximum leadership (Fig3E, right). Furthermore, the increase was observed regardless of the leadership status (leader or follower) when injected with vehicle. In contrast, when both mice received muscimol infusion (cohort #1), the % maximum leadership did not change (Fig3C, right).

The input from vHPC to the amygdala is necessary for context-dependent control of cued fear (45, 46). The hippocampal-amygdala axons originate primarily from the CA1 and subicular neurons in the temporal/caudal half of the Ammon Horn, which includes the ventral and intermediate hippocampus (here collectively referred to as ventral hippocampus) (47, 48). To test whether these axons are necessary for the social synchronization of freezing, we chemogenetically suppressed their terminals in the amygdala. Whole-cell recording confirmed the effectiveness of such suppression, using amygdala slices from mice co-injected with AAV-hSyn-hM4Di-mCherry and AAV-hSynChronos-GFP in the hippocampus. One μM CNO in the bath suppressed EPSCs evoked in the BLA neurons by blue light pulses by 90.4±3.8 % (Fig4A).

For behavioral testing, we injected mice with AAV-hSyn-hM4Di-mCherry in the ventral hippocampus (Fig4C), 25-30 days later implanted cannulas for CNO infusion in the basolateral amygdala (BLA) and allowed mice to recover for 14-17 days.

All dyads were tested twice, at 24h (TEST1) and 72h (TEST2) after training. Forty min before each test, mice received CNO or vehicle infusion in BLA in counterbalanced order (Fig4B). The infusions were counterbalanced because repeated testing *per se* caused fear extinction in some cohorts, although it did not affect synchrony (FigS11). In males, CNO decreased synchrony but had no effect on % freezing (Fig4D upper) or the duration or number of freezing bouts (Fig

S10). Synchrony also did not correlate with freezing measures (FigS9). In females, CNO decreased synchrony and freezing (Fig4E upper). It also decreased the duration of freezing bouts but not the bouts number (FigS10). Despite the strong effect of CNO on both synchrony and freezing in females, synchrony only correlated with % freezing in the low freezers, and the correlation was weak (R^2=0.18, p=0.03, FigS9). To control for non-specific effects of CNO, separate groups of mice underwent the same procedures, except they received AAV-hSyn-GFP (6 male dyads) or AAV-hSyn-Chronos-GFP (4 male and all female dyads). CNO had no effect on synchrony or freezing, and there was no correlation between synchrony and freezing measures, even in the female group (Fig4D, E lower, FigS9). In all cohorts in DREADD disconnection and muscimol inactivation experiments, synchrony and freezing did not change significantly between the first and second halves of the session (FigS13).

Discussion

The main goal of this work was to establish a mouse paradigm and a quantitative measure for social synchronization of an affective behavior. The key findings are that freely interacting mice synchronize freezing response to an auditory conditioned stimulus and the ventral hippocampus to amygdala pathway is required for this synchronization.

Most studies on behavioral synchrony focus on rhythmic movements. They define synchrony as the degree of congruence between behavioral cycles of two subjects (49) and quantify it by coherence and cross-correlation (7, 8, 10, 50).

Such metrics are not applicable in this study because of limited sampling: testing of conditioned fear is limited to a few minutes and not repeatable multiple times. The resulting small number of freezing bouts is insufficient for evaluating rhythmicity or periodicity. Therefore, we defined synchrony more broadly, as simultaneous affect (51) and operationally as simultaneous behavior (49). We quantified synchrony based on the duration of simultaneous freezing or freezing overlap. Because there is, however, always some overlap occurring by chance, which

increases with higher freezing, we calculated freezing synchrony as the difference between the observed freezing overlap and the freezing overlap by chance, normalized to the standard deviation of the chance overlap. This metric factors out the chance overlap and allows comparison among dyads with different levels of freezing. In fact, throughout this study, synchrony in most cohorts did not correlate with freezing measures, which included the % freezing average of dyad members, % freezing of the high and low freezer, % freezing difference between dyad members, and duration or number of freezing bouts. It suggests that most animals respond to social cues and coordinate behavior independently from the level of fear. As an exception, in some but not all female cohorts, synchrony correlated with freezing of the low freezer and with duration of freezing bouts but the correlation was weak. Nevertheless, they suggest differences in how males and females integrate social and emotional information.

While both sexes synchronized freezing, males synchronized it more than females, suggesting sex differences within the circuits involved in synchronization. One mouse study reported lower sociability of females (52), which could explain the lower synchrony. However, other studies did not detect sex differences in the sociability of mice (53, 54), suggesting that sociability and synchrony require separate circuits. The lack of synchrony in most male dyads under infrared light suggest that males rely primarily on vision; whereas the ability to synchronize in most females suggests that females can use other sensory modalities. On the other hand, the freezing level under IR was lower for both sexes. It may result from fear reduction and (or) a switch from passive (freezing) to active (escape) threat response (55). Therefore, the sex differences in synchrony under IR may arise at the fear expression level, not only from the different reliance on vision.

Fear synchrony did not require dmPFC, similar to dmPFC-independence of social motivation in mice (56, 57), although, in a rat study, dmPFC was found necessary for social motivation (58). Meanwhile, dmPFC-dependent social cognition drives empathy-like behavior and hierarchy formation (59). Perhaps, social motivation and synchrony are evolutionary older,

making them less dependent on the prefrontal cortex. However, our study does not rule out that dmPFC modulates fear synchrony, same as it modulates social motivation (59).

Inactivation of the vHPC or its terminals inside the amygdala disrupted fear synchrony. Given the reports of the hippocampal involvement in the attention process (60) and, in particular, the role of the ventral hippocampus in the attention tasks in rodents (61), the impaired synchrony can arise from the loss of attention. Furthermore, the recently discovered “social neurons” in the ventral hippocampus (62) can participate in social attention, potentially encode conspecific information and route it to the amygdala.

Notably, vHPC inactivation or disconnection from the amygdala did not change the overall freezing level but diminished synchronization. It suggests that the role of the social neurons is to adjust the temporal pattern of amygdala activity but not its level. Two types of hippocampal commands, which initiate and terminate freezing, could provide such temporal adjustments. The reported parallel pathways, excitatory hippocampal-amygdala input to the basal and central nuclei (46, 47), and GABAergic input to the basal amygdala (63, 64) might transmit the opposing commands.

Our analysis of the leader-follower relationship revealed that most dyads did not have fixed leaders driving the transitions in and out of freezing; instead, the leadership is flexible, and dyad members followed each another. However, when vHPC was inactivated in only one mouse in a dyad, the treated mouse increased the leadership, suggesting that the vHPC is required for the ability to follow the partner.

Interestingly, the contextual freezing showed no synchronization. One hypothesis is that the contextual fear circuitry lacks the mechanism for the accurate timing of events. Indeed, BNST, which is required for contextual fear expression, mediates fear responses when the timing of an aversive event is uncertain (65-67); therefore, it is unlikely to respond precisely to the partner’s behavioral transitions. Another hypothesis is based on two facts: testing context fear activates dHPC (68-70), and dHPC strongly projects to vHPC through the longitudinal pathway via CA2

(71-73). The activated dHPC may interfere with vHPC from processing social cues via the CA2 route.

Overall, this study adds one additional example to the list of synchronized behaviors in several species (74), the conditioned freezing in mice, and opens up studies of synchronized behaviors in mice.

Acknowledgemens

This work was supported by the NIH grants MH120290 and MH118604 to A.M.

Disclosures

All authors report no biomedical financial interests or potential conflicts of interest.

References

1. Herbert-Read JE (2016): Understanding how animal groups achieve coordinated movement. *J Exp Biol*. 219:2971-2983.
2. Bazazi S, Pfennig KS, Handegard NO, Couzin ID (2012): Vortex formation and foraging in polyphenic spadefoot toad tadpoles. *Behav Ecol Sociobiol*. 66:879-889.
3. Codling EA, Pitchford JW, Simpson SD (2007): Group navigation and the "many-wrongs principle" in models of animal movement. *Ecology*. 88:1864-1870.
4. Seeley TD, Buhrman SC (1999): Group decision making in swarms of honey bees. *Behav Ecol Sociobiol*. 45:19-31.
5. Grunbaum D (1998): Schooling as a strategy for taxis in a noisy environment. *Evol Ecol*. 12:503-522.
6. Duranton C, Gaunet F (2016): Behavioural synchronization from an ethological perspective: Overview of its adaptive value. *Adapt Behav*. 24:181-191.
7. Kupper Z, Ramseyer F, Hoffmann H, Tschacher W (2015): Nonverbal Synchrony in Social Interactions of Patients with Schizophrenia Indicates Socio-Communicative Deficits. *PloS one*. 10.
8. Ramseyer F, Ebert A, Roser P, Edel MA, Tschacher W, Brune M (2020): Exploring nonverbal synchrony in borderline personality disorder: A double-blind placebo-controlled study using oxytocin. *Br J Clin Psychol*. 59:186-207.
9. Curioni A, Minio-Paluello I, Sacheli LM, Candidi M, Aglioti SM (2017): Autistic traits affect interpersonal motor coordination by modulating strategic use of role-based behavior. *Mol Autism*. 8.
10. Georgescu AL, Koeroglu S, Hamilton AFC, Vogeley K, Falter-Wagner CM, Tschacher W (2020): Reduced nonverbal interpersonal synchrony in autism spectrum disorder independent of partner diagnosis: a motion energy study. *Mol Autism*. 11:11.
11. McNaughton KA, Redcay E (2020): Interpersonal Synchrony in Autism. *Current psychiatry reports*. 22:12.
12. Rennung M, Goritz AS (2016): Prosocial Consequences of Interpersonal Synchrony: A Meta-Analysis. *Z Psychol*. 224:168-189.
13. Wiltermuth SS, Heath C (2009): Synchrony and cooperation. *Psychol Sci*. 20:1-5.
14. Swanson HH, Schuster R (1987): Cooperative Social Coordination and Aggression in Male Laboratory Rats - Effects of Housing and Testosterone. *Hormones and behavior*. 21:310-330.
15. Bowen MT, Keats K, Kendig MD, Cakic V, Callaghan PD, McGregor LS (2012): Aggregation in quads but not pairs of rats exposed to cat odor or bright light. *Behav Process*. 90:331-336.
16. Bowen MT, McGregor IS (2014): Oxytocin and vasopressin modulate the social response to threat: a preclinical study. *The international journal of neuropsychopharmacology / official scientific journal of the Collegium Internationale Neuropsychopharmacologicum*. 17:1621-1633.
17. Bowen MT, Kevin RC, May M, Staples LG, Hunt GE, McGregor IS (2013): Defensive aggregation (huddling) in Rattus norvegicus toward predator odor: individual differences, social buffering effects and neural correlates. *PloS one*. 8:e68483.
18. Kim J, Kim C, Han HB, Cho CJ, Yeom W, Lee SQ, et al. (2020): A bird's-eye view of brain activity in socially interacting mice through mobile edge computing (MEC). *Science Advances*. 6.
19. Izhar R, Eilam D (2010): Together they stand: A life-threatening event reduces individual behavioral variability in groups of voles. *Behavioural brain research*. 208:282-285.

20. Eilam D, Zadicario P, Genossar T, Mort J (2012): The anxious vole: the impact of group and gender on collective behavior under life-threat. *Behav Ecol Sociobiol*. 66:959-968.
21. Rabi C, Zadicario P, Mazon Y, Wagner N, Eilam D (2017): The response of social and non-social rodents to owl attack. *Behav Ecol Sociobiol*. 71.
22. Jeon D, Kim S, Chetana M, Jo D, Ruley HE, Lin SY, et al. (2010): Observational fear learning involves affective pain system and Cav1.2 Ca2+ channels in ACC. *Nat Neurosci*. 13:482-488.
23. Ito W, Erisir A, Morozov A (2015): Observation of Distressed Conspecific as a Model of Emotional Trauma Generates Silent Synapses in the Prefrontal-Amygdala Pathway and Enhances Fear Learning, but Ketamine Abolishes those Effects. *Neuropsychopharmacology : official publication of the American College of Neuropsychopharmacology*. 40:2536-2545.
24. Morozov A, Ito W (2019): Social modulation of fear: Facilitation vs buffering. *Genes, brain, and behavior*. 18:e12491.
25. Allsop SA, Wichmann R, Mills F, Burgos-Robles A, Chang CJ, Felix-Ortiz AC, et al. (2018): Corticoamygdala Transfer of Socially Derived Information Gates Observational Learning. *Cell*. 173:1329-1342 e1318.
26. Chen Q, Panksepp JB, Lahvis GP (2009): Empathy is moderated by genetic background in mice. *PloS one*. 4:e4387.
27. Langford DJ, Crager SE, Shehzad Z, Smith SB, Sotocinal SG, Levenstadt JS, et al. (2006): Social modulation of pain as evidence for empathy in mice. *Science*. 312:1967-1970.
28. Pan BX, Vautier F, Ito W, Bolshakov VY, Morozov A (2008): Enhanced cortico-amygdala efficacy and suppressed fear in absence of Rap1. *The Journal of neuroscience : the official journal of the Society for Neuroscience*. 28:2089-2098.
29. Ito W, Morozov A (2019): Prefrontal-amygdala plasticity enabled by observational fear. *Neuropsychopharmacology : official publication of the American College of Neuropsychopharmacology*. 44:1778-1787.
30. Stachniak TJ, Ghosh A, Sternson SM (2014): Chemogenetic synaptic silencing of neural circuits localizes a hypothalamus-->midbrain pathway for feeding behavior. *Neuron*. 82:797-808.
31. Morozov A, Sukato D, Ito W (2011): Selective suppression of plasticity in amygdala inputs from temporal association cortex by the external capsule. *The Journal of neuroscience : the official journal of the Society for Neuroscience*. 31:339-345.
32. Ho J, Tumkaya T, Aryal S, Choi H, Claridge-Chang A (2019): Moving beyond P values: data analysis with estimation graphics. *Nature methods*. 16:565-566.
33. Warthen DM, Wiltgen BJ, Provencio I (2011): Light enhances learned fear. *Proc Natl Acad Sci U S A*. 108:13788-13793.
34. Li Z, Lu YF, Li CL, Wang Y, Sun W, He T, et al. (2014): Social interaction with a cagemate in pain facilitates subsequent spinal nociception via activation of the medial prefrontal cortex in rats. *Pain*. 155:1253-1261.
35. Hitti FL, Siegelbaum SA (2014): The hippocampal CA2 region is essential for social memory. *Nature*. 508:88-92.
36. Okuyama T, Kitamura T, Roy DS, Itohara S, Tonegawa S (2016): Ventral CA1 neurons store social memory. *Science*. 353:1536-1541.
37. Phillips ML, Robinson HA, Pozzo-Miller L (2019): Ventral hippocampal projections to the medial prefrontal cortex regulate social memory. *Elife*. 8.
38. Sierra-Mercado D, Padilla-Coreano N, Quirk GJ (2010): Dissociable roles of prelimbic and infralimbic cortices, ventral hippocampus, and basolateral amygdala in the expression and extinction of conditioned fear. *Neuropsychopharmacology : official publication of the American College of Neuropsychopharmacology*. 36:529-538.
39. Izquierdo I, Furini CR, Myskiw JC (2016): Fear Memory. *Physiological reviews*. 96:695-750.

40. Giustino TF, Maren S (2015): The Role of the Medial Prefrontal Cortex in the Conditioning and Extinction of Fear. *Frontiers in behavioral neuroscience*. 9:298.
41. Ortiz S, Latsko MS, Fouty JL, Dutta S, Adkins JM, Jasnow AM (2019): Anterior Cingulate Cortex and Ventral Hippocampal Inputs to the Basolateral Amygdala Selectively Control Generalized Fear. *The Journal of neuroscience : the official journal of the Society for Neuroscience*. 39:6526-6539.
42. Laurent V, Westbrook RF (2009): Inactivation of the infralimbic but not the prelimbic cortex impairs consolidation and retrieval of fear extinction. *Learn Mem*. 16:520-529.
43. Holt W, Maren S (1999): Muscimol inactivation of the dorsal hippocampus impairs contextual retrieval of fear memory. *The Journal of neuroscience : the official journal of the Society for Neuroscience*. 19:9054-9062.
44. Quinn JJ, Wied HM, Ma QD, Tinsley MR, Fanselow MS (2008): Dorsal hippocampus involvement in delay fear conditioning depends upon the strength of the tone-footshock association. *Hippocampus*. 18:640-654.
45. Orsini CA, Kim JH, Knapska E, Maren S (2011): Hippocampal and prefrontal projections to the basal amygdala mediate contextual regulation of fear after extinction. *The Journal of neuroscience : the official journal of the Society for Neuroscience*. 31:17269-17277.
46. Xu C, Krabbe S, Grundemann J, Botta P, Fadok JP, Osakada F, et al. (2016): Distinct Hippocampal Pathways Mediate Dissociable Roles of Context in Memory Retrieval. *Cell*. 167:961-972 e916.
47. Kishi T, Tsumori T, Yokota S, Yasui Y (2006): Topographical projection from the hippocampal formation to the amygdala: a combined anterograde and retrograde tracing study in the rat. *The Journal of comparative neurology*. 496:349-368.
48. Fanselow MS, Dong HW (2010): Are the dorsal and ventral hippocampus functionally distinct structures? *Neuron*. 65:7-19.
49. Bernieri FJ, Reznick JS, Rosenthal R (1988): Synchrony, Pseudosynchrony, and Dissynchrony - Measuring the Entrainment Process in Mother Infant Interactions. *J Pers Soc Psychol*. 54:243-253.
50. Jiang Y, Platt ML (2018): Oxytocin and vasopressin flatten dominance hierarchy and enhance behavioral synchrony in part via anterior cingulate cortex. *Sci Rep*. 8:8201.
51. Siegman AW, Reynolds, M. (1982): Interviewer-interviewee nonverbal communications: An interactional approach. In: Davis M, editor. *Interaction rhythms: Periodicity in communicative behavior*. New York: Human Sciences Press, pp 249-277.
52. Defensor EB, Pearson BL, Pobbe RL, Bolivar VJ, Blanchard DC, Blanchard RJ (2011): A novel social proximity test suggests patterns of social avoidance and gaze aversion-like behavior in BTBR T+ tf/J mice. *Behavioural brain research*. 217:302-308.
53. Silverman JL, Tolu SS, Barkan CL, Crawley JN (2010): Repetitive self-grooming behavior in the BTBR mouse model of autism is blocked by the mGluR5 antagonist MPEP. *Neuropsychopharmacology : official publication of the American College of Neuropsychopharmacology*. 35:976-989.
54. Yang M, Clarke AM, Crawley JN (2009): Postnatal lesion evidence against a primary role for the corpus callosum in mouse sociability. *The European journal of neuroscience*. 29:1663-1677.
55. Mongeau R, Miller GA, Chiang E, Anderson DJ (2003): Neural correlates of competing fear behaviors evoked by an innately aversive stimulus. *The Journal of neuroscience : the official journal of the Society for Neuroscience*. 23:3855-3868.
56. Avale ME, Chabout J, Pons S, Serreau P, De Chaumont F, Olivo-Marin JC, et al. (2011): Prefrontal nicotinic receptors control novel social interaction between mice. *Faseb Journal*. 25:2145-2155.

57. Yizhar O, Fenno LE, Prigge M, Schneider F, Davidson TJ, O'Shea DJ, et al. (2011): Neocortical excitation/inhibition balance in information processing and social dysfunction. *Nature*. 477:171-178.
58. Rudebeck PH, Walton ME, Millette BH, Shirley E, Rushworth MF, Bannerman DM (2007): Distinct contributions of frontal areas to emotion and social behaviour in the rat. *The European journal of neuroscience*. 26:2315-2326.
59. Bicks LK, Koike H, Akbarian S, Morishita H (2015): Prefrontal Cortex and Social Cognition in Mouse and Man. *Front Psychol*. 6:1805.
60. Aly M, Turk-Browne, N.B. (2017): How Hippocampal Memory Shapes, and Is Shaped by, Attention. In: Hannula D, Duff, M., editor. *The Hippocampus from Cells to Systems*: Springer, Cham.
61. Li X, Chen W, Pan K, Li H, Pang P, Guo Y, et al. (2018): Serotonin receptor 2c-expressing cells in the ventral CA1 control attention via innervation of the Edinger-Westphal nucleus. *Nat Neurosci*. 21:1239-1250.
62. Rao RP, von Heimendahl M, Bahr V, Brecht M (2019): Neuronal Responses to Conspecifics in the Ventral CA1. *Cell Rep*. 27:3460-3472 e3463.
63. Lubkemann R, Eberhardt J, Rohl FW, Janitzky K, Nullmeier S, Stork O, et al. (2015): Identification and Characterization of GABAergic Projection Neurons from Ventral Hippocampus to Amygdala. *Brain Sci*. 5:299-317.
64. McDonald AJ, Mott DD (2017): Functional neuroanatomy of amygdalohippocampal interconnections and their role in learning and memory. *J Neurosci Res*. 95:797-820.
65. Goode TD, Maren S (2017): Role of the bed nucleus of the stria terminalis in aversive learning and memory. *Learn Mem*. 24:480-491.
66. Goode TD, Ressler RL, Acca GM, Miles OW, Maren S (2019): Bed nucleus of the stria terminalis regulates fear to unpredictable threat signals. *Elife*. 8.
67. Haufler D, Nagy FZ, Pare D (2013): Neuronal correlates of fear conditioning in the bed nucleus of the stria terminalis. *Learn Mem*. 20:633-641.
68. Maviel T, Durkin TP, Menzaghi F, Bontempi B (2004): Sites of neocortical reorganization critical for remote spatial memory. *Science*. 305:96-99.
69. Squire LR, Genzel L, Wixted JT, Morris RG (2015): Memory consolidation. *Cold Spring Harb Perspect Biol*. 7:a021766.
70. Preston AR, Eichenbaum H (2013): Interplay of hippocampus and prefrontal cortex in memory. *Current biology : CB*. 23:R764-773.
71. Kohara K, Pignatelli M, Rivest AJ, Jung HY, Kitamura T, Suh J, et al. (2014): Cell type-specific genetic and optogenetic tools reveal hippocampal CA2 circuits. *Nat Neurosci*. 17:269-279.
72. Tamamaki N, Abe K, Nojyo Y (1988): Three-dimensional analysis of the whole axonal arbors originating from single CA2 pyramidal neurons in the rat hippocampus with the aid of a computer graphic technique. *Brain research*. 452:255-272.
73. Meira T, Leroy F, Buss EW, Oliva A, Park J, Siegelbaum SA (2018): A hippocampal circuit linking dorsal CA2 to ventral CA1 critical for social memory dynamics. *Nat Commun*. 9:4163.
74. Duranton C, Bedossa T, Gaunet F (2017): Interspecific behavioural synchronization: dogs exhibit locomotor synchrony with humans. *Sci Rep*. 7:12384.

Figure legends

Figure 1. Synchronization of auditory fear differs between sexes and relies on vision more strongly in males than in females. A) Scheme for testing fear synchrony. Fear conditioning training on day 1 and testing on day 2. Blue rectangles and red vertical bars represent CS and US, respectively. **B)** Examples of freezing timelines in dyads with high (upper, synchrony=3.4) and low (lower, 0.14) freezing synchrony. CS onsets at 60 s are zoomed in. Freezing bouts of animal 1 and 2 are shown in blue and orange, and freezing overlaps in green. **C)** Computing freezing synchrony. The observed freezing overlap L is taken from the freezing timelines. The timelines are then randomly permutated 1000 times, giving 1000 permutated overlaps, from which the mean chance overlap C and the standard deviation SD are calculated. SYNCHRONY = (L-C) / SD. **D)** Summary diagrams for synchrony in male and female dyads tested under visible or infrared lights. Independent dyads were tested under visible and infrared light. Horizontal bars indicate means±SEM. The visible synchrony panel (left) includes the effect size as a bootstrap 95% confidence interval (CI, vertical line) and the resampled distribution of the mean difference (orange) computed by DABEST(32). The effect size is aligned with the mean of the female test groups. Under the visible light, synchrony was significant in both sexes (one-sample t-test: males: $p<0.0001$, n=17, females: $p=0.002$, n=16) and higher in males (two-sample t-test: $p=0.007$). Under the infrared light, synchrony was not significant in males (Wilcoxon signed-rank test: n=14) but significant in females (one-sample t-test: $p<0.05$, n=14). One-sample t-test: * $p<0.05$, ** $p<0.01$, **** $p<0.0001$, two-sample t-test: $^{\#\#}$ $p<0.01$. **E-H)** Scatter plots of synchrony vs. freezing in males under visible light (E), males under infrared light (F), females under visible light (G), and

females under infrared light (H). Freezing (%) is the average of two mice in each dyad. No significant correlation was found.

Figure 2. Fear synchrony requires the ventral hippocampus. A) Experimental timeline. Independent dyads were infused with vehicle or muscimol. **B, E, H)** Examples of dye injections in the muscimol inactivation sites in the dmPFC (B), dHPC (E), and vHPC (H). **C, F, I)** Summary diagrams for synchrony (left) and % freezing average (right) in dyads with both mice injected in dmPFC (C) (n=9/10 with vehicle/muscimol), dHPC (F) (n=8/7), and vHPC (I) (n=8/8). For synchrony, comparisons to 0 were made by the one-sample t-test in C and Wilcoxon signed-rank test in F and I. For synchrony and freezing average, comparisons between groups were made by the two-sample t-test in C and Mann-Whitney test in F and I. * $p<0.05$, $^{\#}$ $p<0.05$, ** $p<0.01$, $^{\#\#}$ $p<0.01$, *** $p<0.001$. Horizontal bars indicate means±SEM. The resampled distribution of the mean difference (orange) and the 95% confidence interval (vertical line) are shown on the right. The effect size is aligned with the mean of the test group (muscimol). **D, G, J)** Scatter plots of synchrony vs. freezing for the dmPFC (D), dHPC (G), and vHPC (J) inactivation experiments. Freezing (%) is the average of two mice in each dyad. No significant correlation was found.

Figure 3. Ventral hippocampal is required for synchrony and suppresses leadership. A) Experimental scheme of behavioral testing with muscimol suppression. **B, D)** Left: Schematics of muscimol injections. Right: Summary diagrams of synchrony (left), % freezing averages of both dyad members (middle), and freezing-synchrony scatter plot (right). No significant correlation was found. Open and black circles represent dyads infused with vehicle and muscimol, respectively (n=10 (B), 11 dyads (C)). **C, E)** Left and middle: Trajectories of the absolute leadership bias along the matched transitions. Dashed lines represent dyads with the % maximum leadership above 30%. Right: % maximum leadership after infusion of vehicle and muscimol. The gray shades

represent the >30% and <-30% cutoffs. Connected data points represent the same dyad. Positive and negative % maximum leadership indicates that animal #1 or #2 exhibited stronger leadership, respectively. In C, #1 and #2 were assigned arbitrarily. In E, #1 was assigned to the animal receiving infusions. Wilcoxon matched-pairs test: * $p<0.05$. The resampled mean difference distribution (orange) and the 95% confidence interval (vertical line) are shown. The effect size is aligned with the mean of the test group (muscimol).

Figure 4. Fear synchrony requires the ventral hippocampal input to the amygdala. A) DREADD suppression of the ventral hippocampal terminals in BLA *ex vivo*. Left: schematics of viral injection, ex vivo stimulation, and whole-cell recording. Middle: example of EPSC evoked in a BLA neuron by blue light stimulation of the vHPC terminals in the absence of CNO (black), and after 10 min of perfusion with 1 μM CNO (red), shown as averages of 5 consecutive sweeps. Right: summary of EPSC changes (no CNO vs. CNO), recorded from 5 BLA neurons, and % suppression by 1 μM CNO. Wilcoxon signed-rank test: #### $p<0.0001$. Horizontal bars indicate means±SEM. **B)** Experimental scheme of behavioral testing with DREADD suppression. **C)** Left: Schematics of viral injection and cannula placement. Right: Fluorescent images of the hippocampal (vHPC) and amygdala (AMYG) slices from mice injected with AAV-hSyn-hM4Di-mCherry (upper row) and AAV-hSyn-GFP (lower row) in the ventral/intermediate hippocampus. **D, E)** Summary diagrams (males in D, females in E) of synchrony (left), % freezing average (middle), and freezing-synchrony scatter plot (right) in the dyads expressing hM4Di-mCherry (upper row, DREADD disconnection, n=13 (male), 12 (female)) or GFP or Chronos-GFP (lower row, CNO/virus controls, n=10 (male), 11 (female)), both mice in the dyad infused with vehicle (open circle) or 3 μM CNO (black filled circle) in the amygdala. No significant correlation was found in DE, most right column. The connected data points represent the same dyads. Freezing (%) is the average of two mice in each dyad. Wilcoxon matched-pairs test: * $p<0.05$, ** $p<0.01$.

The resampled mean difference distribution (orange) and the 95% confidence interval (vertical line) are shown. The effect size is aligned with the mean of the test group (CNO).

KEY RESOURCES TABLE

Resource Type	Specific Reagent or Resource	Source or Reference	Identifiers	Additional Information
Add additional rows as needed for each resource type	Include species and sex when applicable.	Include name of manufacturer, company, repository, individual, or research lab. Include PMID or DOI for references; use “this paper” if new.	Include catalog numbers, stock numbers, database IDs or accession numbers, and/or RRIDs. RRIDs are highly encouraged; search for RRIDs at https://scicrunch.org/resources.	Include any additional information or notes if necessary.
Chemical Compound or Drug	muscimol	Tocris	catalog: 0298	
Organism/strain	C57BL/6N male mice	The Jackson Laboratory	RRID:IMSR_JAX:005304	
Organism/strain	129SvEv female mice	Taconic	catalog: 129SVE-F	
Recombinant DNA	pAAV-hSyn-EGFP	a gift from Bryan Roth	RRID:Addgene_50465	
Recombinant DNA	pAAV-hSyn-hM4D(Gi)-mCherry	a gift from Bryan Roth	RRID:Addgene_50475	
Recombinant DNA	pAAV-Syn-Chronos-GFP	a gift from Edward Boyden	RRID:Addgene_59170	
Software; Algorithm	Videoplay annotation tool	this paper	https://github.com/wataruito/codes_in_Emotional_sync_Ito_et_al	

Key Resource Table